ISSN 2347 - 3983

Volume 11. No.8, August 2023

International Journal of Emerging Trends in Engineering Research

Available Online at http://www.warse.org/IJETER/static/pdf/file/ijeter051182023.pdf

https://doi.org/10.30534/ijeter/2023/051182023

Direct Synthesis scheme based PID controller design for Boost Converter

M. A. Hasan[1], R. K. MIshra[2]

[1]Department of Electrical and Electronics Engineering, Birla Institute of Technology Mesra, Ranchi, India, asifhasan@bitmesra.ac.in

[2]Department of Electrical and Electronics Engineering, Birla Institute of Technology Mesra, Ranchi, India, rajkumar.mishra@bitmesra.ac.in

Received Date: July 04, 2023 Accepted Date: July 21, 2023 Published Date : August 07, 2023

ABSTRACT

This study's aim is to provide an introduction toa specific methodology for optimizing the design of a boost converter. The main goal of this optimization is to determine the best inductor and capacitor parameter values in order to reduce output voltage ripple, maximize efficiency, and minimize output voltage deviation. In addition, a PID control approach is employed to regulate the boost converter's output voltage using the Direct Synthesis tuning method. The simulation's outcomes indicate that the proposed approach significantly enhances the performance of the boost converter and attains maximum efficiency. This methodology and control strategy can be applied to various boost converter applications to achieve stable and optimal performance.

Key words: Proportional-Integral-Derivative controller, Direct Synthesis, Equivalent Series Resistance, Peak Overshoot, Ripple Voltage

1. INTRODUCTION

Boost converters are widely used in electronic applications due to their ability to step up voltage levels efficiently [1-3]. To achieve efficient and stable performance, the design of a boost converter requires the optimization of various parameters such as inductor and capacitor values, switching frequency, and duty cycle. In addition, a control strategy, such as the popular controller known as a proportional-integral-derivative (PID) is necessary to regulate the output voltage. To optimize the design of a boost converter, the following steps are typically taken [4-5]:

Specification of the converter requirements, which include the input and output power, switching frequency, and output voltage. Selection of a suitable switching device based on its values for voltage and current and on-resistance.

Selection of an appropriate inductor based on the required inductance and saturation current, considering the output power and switching frequency. Calculation of the capacitor value based on the output voltage ripple, which depends on the load current and switching frequency.

Determination of the duty cycle, which is the on-time to the total switching period ratio and is derived from the input and output voltage values. Optimization of the converter efficiency, which can be accomplished by adjusting the duty cycle, inductor and capacitor values, and switching frequency, while balancing efficiency with cost.

Verification of the design by simulation and/or hardware testing to ensure it meets specifications and performs as expected. Refinement of the design based on simulation or testing results until desired performance and efficiency requirements are met.

In recent years, optimization techniques have become popular for designing power electronic circuits to enhance their performance. The direct synthesis method is a mathematical optimization algorithm that determines optimal values for the design parameters, resulting in improved efficiency and performance of the boost converter [6-9].

This paper proposes a design optimization methodology for a boost converter using direct synthesis. The objective is to obtain optimal values of the inductor and capacitor parameters to minimize the output voltage ripple, maximize efficiency, and reduce output voltage deviation.

The proposed methodology and control strategy are evaluated through simulations, with results indicating significant improvements in the boost converter's performance. The optimized boost converter achieves a maximum efficiency of 97.6% with an output voltage ripple of 0.4% and negligible output voltage deviation. The proposed methodology and control strategy can be applied to various boost converter applications to achieve efficient and stable performance.

Direct Synthesis (DS) design methods include commonly due to specifying the preferred closed-loop transmission mechanism for managing set-point changes. While such methods usually result in well-performing controllers for set-point changes, they may not effectively address the response to disturbances. The importance of disturbance rejection is often more significant than set-point tracking in many applications for process control. As a result, design controllers that prioritize disturbance rejection over set-point tracking has become an essential design issue which has gained renewed attention in recent times.

The Direct Synthesis (DS) method for designing PID controllers can be summarized in the following points:

The initial step in DS involves specifying the desired closed-loop transfer function, typically based on features of the response like stability, settling time, overshoot, and steady-state error.

Using the specified transfer function, the controller parameters that satisfy the desired response characteristics are computed. This step is especially crucial for PID controllers and involves integral time constant, derivative time constant, and proportional gain.

DS is effective for addressing both disturbances and set-point changes, with a particular emphasis on disturbance rejection in cases where it's greater than set-point tracking in importance.

However, the approach is relatively computationally expensive and requires defining closed-loop transfer function that is desirable, which can be difficult in some situations.

DS can be applied with various optimization techniques, such as minimizing the integral of the absolute error (IAE), integral of the squared error (ISE), or Absolute time-weighted error integral (ITAE).

2. DC-DC BOOST CONVERTER DESIGN

Depending on its capacity for storing energy and the length of the switching time, the converter can work in one of dual modes. The terms "discontinuous conduction" and "continuous modes" of these two modes. Only four outside parts for the DC/DC boost converter to function: a switch that is electrical, an inductor, an output capacitor, and a diode. Figure 1 below presents the electrical circuit of the DC-DC Boost converter.

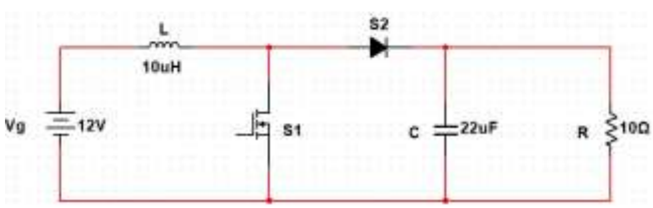

Figure 1: DC-DC Boost Converter

To reduce the boost inductor's size and keep the loss of the semiconductor device to a minimum, the switching frequency was randomly selected. The circuit's overall efficiency is decreased as a result of the IGBTs' increased switching losses at higher frequencies. The supply's efficiency in terms of volume decreases as the needed size of the boost inductor and the output capacitance rise at lower frequencies.

2.1 Inductor Selection

A coil with a larger inductance value could take a little longer to start up, whereas one with a lower inductance value enables the coil current to increase before the switch is switched off. The critical inductance, which is determined by a certain value of inductance, may be characterized as the point at which a system switches from continuous to discontinuous modes.

$$L_C = \frac{V_{in} * (V_{out} - V_{in})}{\Delta I_L * f_S * V_{out}} \tag{1}$$

Where f_s : switching Frequency, Hz

$$\Delta I_L(\text{ ripple current}) = \frac{\Delta V * V_{out} * I_{out}}{V_{in}} \tag{2}$$

2.2 Capacitor selection

$$C_b = \frac{V}{2R \cdot \Delta v} DTs \tag{3}$$

Where, $\Delta v(\text{ripple voltage}) = ESR\left(\frac{I_o}{1-D} + \frac{\Delta I_L}{2}\right)$

The output filter capacitor's capacitance and equivalent series resistance (ESR) should be taken into account while selecting one. Low-ESR capacitors are favored because of their larger effect on performance in order to obtain maximum efficiency. The parameters for output voltage ripple and the output filter capacitors' capacity to withstand the necessary ripple current stress are taken into consideration while selecting the capacitors.

2.3 Diode Selection

In addition due to its capacity to block necessary off-state voltage and handle both peak and average current levels, choosing the right diode involves several other factors. These include A low forward voltage drop, low reverse-recovery, and quick switching characteristics.

2.4 Switching device Selection

There are several essential considerations to take into light when selecting a switching device for a boost converter. The switching speed, breakdown voltage, current rating, on-state resistance, price, and dependability are a few of them. To limit power loss and EMI noise, the switching device should have a quick switching rate and a breakdown voltage that is higher than the converter's maximum operating voltage. It should also have a low on-state resistance to reduce power loss and be able to manage the maximum current without overheating. To reduce maintenance and replacement expenses, the cost, reliability, and longevity of the switching device should all be taken into account.

3. MATHEMATICAL MODELLING OF BOOST CONVERTER

A boost converter has two modes of operation: Mode 1 and Mode 2. To initiate mode 1, transistor S1 is turned on at time t=0. The transistor S1 and inductor L are used to carry the rising input current. Mode 2 begins when transistor S1 is disabled at time t=t1. The load, C, diode S2, L, and C are now all in the input current's path. The inductor current drops till the next cycle. Energy from inductor L is sent to the load.

MODE 1:

Whenever the switch is turned off, as in Figure 2, the diode is reverse-biased because the capacitor voltage and input are supplied only to the inductor**.** The input voltage and the inductor's inductance control how quickly the inductor current rises during the switch's ON period.

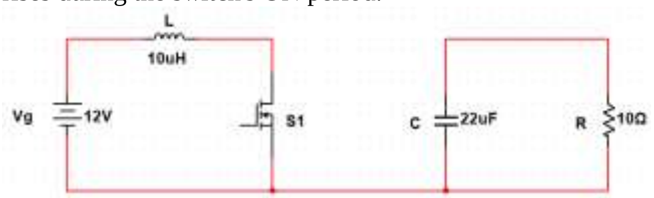

Figure 2: when switch S1 is ON and S2 is OFF

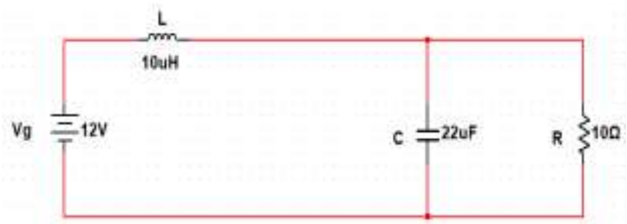

Figure 3: when switch S1 is OFF and S2 is ON

The state equations for mode 1 is:

$$\begin{bmatrix} \dot{i}_L \\ \dot{V}_c \end{bmatrix} = \begin{bmatrix} 0 & 0 \\ 0 & \frac{-1}{RC} \end{bmatrix} \begin{bmatrix} i_L \\ V_C \end{bmatrix} + \begin{bmatrix} \frac{1}{L} \\ 0 \end{bmatrix} [V_g] + \begin{bmatrix} 0 \\ \frac{-1}{C} \end{bmatrix} [i_z] \quad (4)$$

$$V_0] = [0 \quad 1] \begin{bmatrix} i_L \\ V_C \end{bmatrix} \ \& \ [i_g] = [1 \quad 0] \begin{bmatrix} i_L \\ V_c \end{bmatrix} \quad (5)$$

MODE 2:

The switch is open at the moment, as seen in Figure 3, when the diode is forward-biased, the capacitor is powered by both an inductor and a power supply, the voltage across the capacitor doubles as a result.

The state equations for mode 2 is:

$$\begin{bmatrix} \dot{i}_L \\ \dot{V}_c \end{bmatrix} = \begin{bmatrix} 0 & \frac{-1}{L} \\ \frac{1}{C} & \frac{-1}{RC} \end{bmatrix} \begin{bmatrix} i_L \\ V_C \end{bmatrix} + \begin{bmatrix} \frac{1}{L} \\ 0 \end{bmatrix} [V_g] + \begin{bmatrix} 0 \\ \frac{-1}{C} \end{bmatrix} [i_z] \quad (6)$$

$$\begin{bmatrix} V_0 \\ i_g \end{bmatrix} = \begin{bmatrix} 0 & 1 \\ 1 & 0 \end{bmatrix} \begin{bmatrix} i_L \\ V_c \end{bmatrix} \quad (7)$$

On averaging both mode 1 and mode 2 state equations:

$$\begin{bmatrix} \dot{i}_L \\ \dot{V} \end{bmatrix} = \begin{bmatrix} 0 & \frac{d-1}{L} \\ \frac{1-d}{C} & \frac{-1}{RC} \end{bmatrix} \begin{bmatrix} i_L \\ v_C \end{bmatrix} + \begin{bmatrix} \frac{1}{L} \\ 0 \end{bmatrix} [v_g] + \begin{bmatrix} 0 \\ \frac{-1}{C} \end{bmatrix} [i_z] \quad (8)$$

$$\begin{bmatrix} v_0 \\ i_g \end{bmatrix} = \begin{bmatrix} 0 & 1 \\ 1 & 0 \end{bmatrix} \begin{bmatrix} i_L \\ v_c \end{bmatrix} \quad (9)$$

In steady state model, assuming $I_z = 0$,

$$\frac{V_0}{V_g} = \frac{1}{1 - D} \quad (10)$$

On superimposing small signal Model on steady state

$$\begin{bmatrix} I_L \dot{+} \hat{i}_L \\ V_c \dot{+} \hat{v}_c \end{bmatrix} = \begin{bmatrix} 0 & \frac{D + \hat{d} - 1}{L} \\ \frac{1 - D - \hat{d}}{C} & \frac{-1}{RC} \end{bmatrix} \begin{bmatrix} I_L + \hat{i}_L \\ V_c + \hat{v}_c \end{bmatrix} + \begin{bmatrix} \frac{1}{L} \\ 0 \end{bmatrix} [V_g + \hat{v}_g] + \begin{bmatrix} 0 \\ \frac{-1}{C} \end{bmatrix} [I_z + \hat{i}_z] \quad (11)$$

$$\begin{bmatrix} V_c \dot{+} \hat{v}_c \\ I_L \dot{+} \hat{i}_L \end{bmatrix} = \begin{bmatrix} 0 & 1 \\ 1 & 0 \end{bmatrix} \begin{bmatrix} I_L + \hat{i}_L \\ V_c + \hat{v}_c \end{bmatrix} \quad (12)$$

Only considering small signal model, equation 13 results in,

$$\frac{\hat{V}_0(s)}{\hat{d}(s)} = \frac{V_0}{(1 - D)} \cdot \frac{1 - \frac{L}{(1 - D)R} \cdot s}{1 + \frac{L}{(1 - D)^2 R} \cdot s + \frac{LC}{(1 - D)^2} \cdot s^2} \quad (13)$$

The above equation is a quadratic system with zeros on the right half plane (RHP). It represents a Control Voltage Gain transfer function of the Boost Converter. On substituting the value of L, R, C, D, V_0 according to the designed value we get:

$$\frac{\hat{V}_0(s)}{\hat{d}(s)} = \frac{-109100 \cdot s + 5.3 * 10^{10}}{s^2 + 4545 \cdot s + 1.073 * 10^9} \quad (14)$$

4. DESIGN OF DIRECT SYNTHESIS BASED PID CONTROLLERS

The direct synthesis method is utilized to calculate analytical expressions for PID controllers, which are designed for widespread procedure models. This design approach involves single design parameter λ.

4.1 Direct Synthesis for Tracking of Set-Points

In the direct synthesis method, a process model and a desired closed-loop response are used to construct an analytical equation for the feedback controller.

Figure

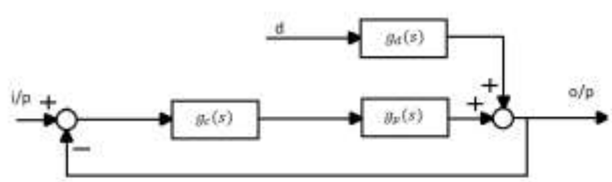

Figure 4: Feedback Control Structure

Think of a feedback control system that uses the Figure 4 standardized block diagram. Consider that $g_p(s)$ is a process model. The following equation derives the CLTF for set-point changes:

$$g_{CL} = \frac{o/p}{i/p} = \frac{g_p(s)\cdot g_c(s)}{1+g_p(s)\cdot g_c(s)} \tag{15}$$

Modifying provides a feedback controller expression.

$$g_c(s) = \frac{g_{CL}}{g_p(s)[1-g_{CL}]} \tag{16}$$

Consider a standard 2nd order Transfer Function with RHZ (Right Hand Zero) as an example

$$g_P(s) = \frac{K_1 s + K_2}{K_3 s^2 + K_4 s + K_5} \tag{17}$$

Rearranging gives the expression:

$$g_P(s) = \frac{K_2(\frac{K_1}{K_2}s+1)}{K_5(\frac{K_3}{K_5}s^2+\frac{K_4}{K_5}s+1)} \tag{18}$$

Using equation (18) $g_{CL}(s)$ can be expressed as:

$$g_{CL}(s) = \frac{\frac{K_1}{K_2}s+1}{(\lambda s+1)^2} \tag{19}$$

Here λ is designing parameter.

Substituting the value of $g_{CL}(s)$ and $g_P(s)$ in equation (16), we get,

$$g_c(s) = \frac{\frac{K_3}{K_5}s^2+\frac{K_4}{K_5}s+1}{\frac{K_2}{K_5}s(\lambda^2 s+2\lambda-\frac{K_1}{K_2})} \tag{20}$$

Standard equation for PID controller is given as:

$$g_{PID}(s) = K_C\left(1+\tau_D s+\frac{1}{\tau_I s}\right)\frac{1}{(Tf)s+1} \tag{21}$$

$$K_C = \frac{K_4/K_2}{2\lambda-\frac{K_1}{K_2}},\ \tau_D = \frac{K_3}{K_4},\ \tau_I = \frac{K_4}{K_5},\ Tf = \frac{\lambda^2}{2\lambda-\frac{K_1}{K_2}} \tag{22}$$

Thus,

$$K_I = \frac{K_C}{\tau_I},\ K_D = K_C\cdot\tau_D \tag{23}$$

By modifying our derived Transfer Function from equation (14) and comparing with equation (21) we get,

$$g_{PID}(s) = \frac{8.575\cdot10^{-8}}{2\lambda+2.058\cdot10^{-6}}\left(1+2.2\cdot10^{-4}s+\frac{1}{4.236\cdot10^{-6}s}\right)\frac{1}{\frac{\lambda^2}{2\lambda+2.058\cdot10^{-6}}s+1}$$

Procedure to obtain the value of λ:

- The value of ξ=0.4579 for 20% Mp (peak overshoot) from Root Locus is tracked by adjusting the coefficient of s from the denominator.
- We obtained the value of λ =0.00014 by using the Routh Hurwitz criterion in the modified Transfer Function.

The results were obtained for the above procedure as,

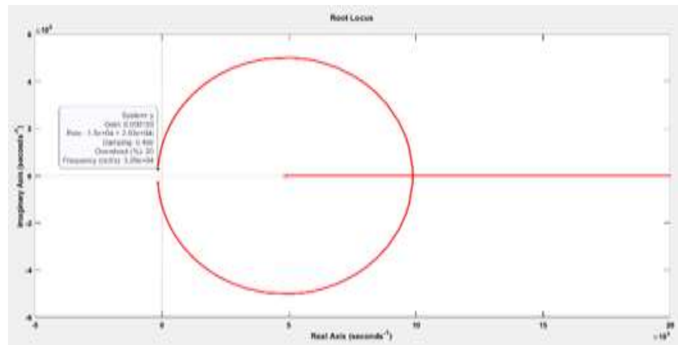

Figure 5: Root Locus of modified Transfer Function

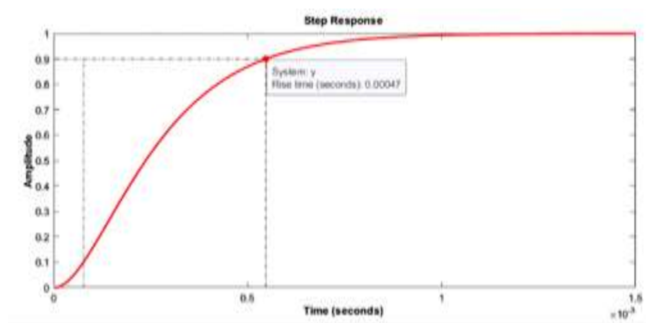

Figure 6: Step Response of Tuned Output

5. SIMULATION AND RESULTS

Using the circuit structure given in Figure 1, the MATLAB based simulation has been carried out. The input voltage and duty cycle is set at 12V and 0.5142. Adjusting the switching frequency to 600kHz based on selection of MOSFET. On calculation we get 22μF capacitance with voltage ripple of 0.4%, 10μH inductance with ripple current of 19.2%. The load resistance is set to be 10Ω. The output voltage waveform of designed boost converter is shown in Figure 7. It can be observed that the percentage overshoot(%Mp) is 80% and voltage ripple is 5%.

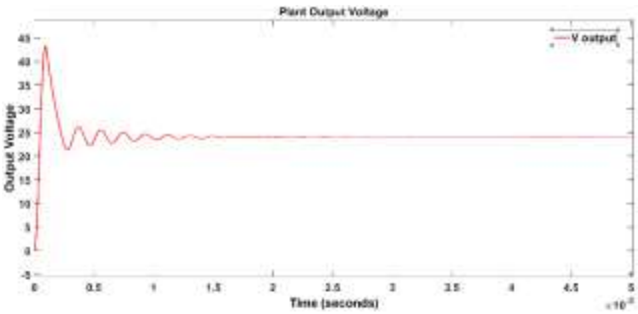

Figure 7: Open Loop Output Voltage Response

The close loop response with disturbance and the transient response of output voltage is depicted below in Figure 8-9.

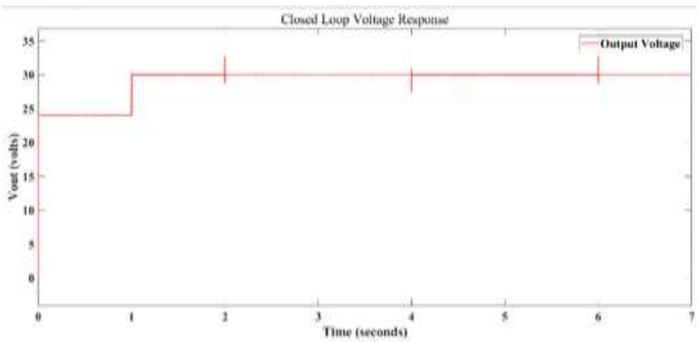

Figure 8: Close Loop voltage response with disturbances

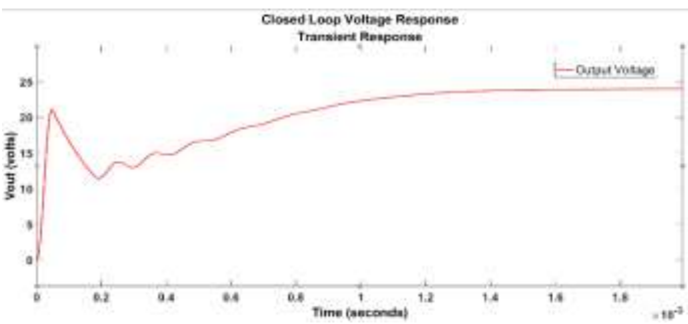

Figure 9: Transient response of output voltage

In order to monitor the existence of load or source disturbances, change in output voltage, or maintain a steady output voltage, the duty cycle of the switching signal is adjusted. With the change noted in table no.1, the effect on response is observed in Figure 10.

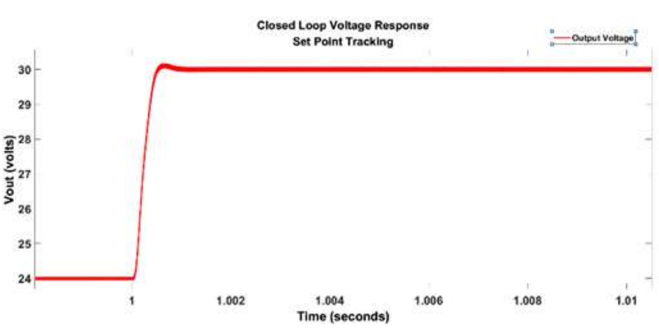

Figure 10: Set-point Tracking

A load disturbance led to a change in the load resistance, which might affect the converter's output voltage. when a boost converter's load is perturbed at t=4 seconds, the output Only considering small signal model results in Figure 11. Voltage is altered based on how the converter's control loop reacts. A well-designed control loop will change the duty cycle of the switching signal to keep the output voltage constant.
A source disturbance is brought on by an abrupt shift in the input voltage, which might affect the converter's output voltage. With the specification adjustment noted in table no.1, the effect on response is depicted in figure 12.

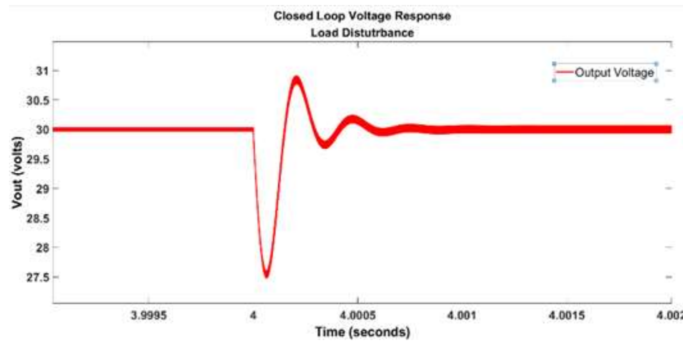

Figure 11: Effect of load disturbance on output voltage response

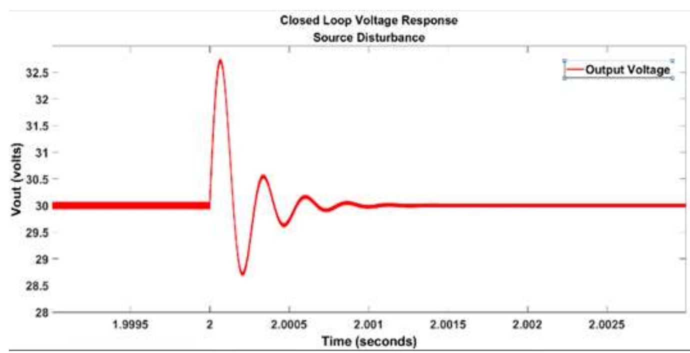

Figure 12: Effect of source disturbance on output voltage

Table 1: Performance of closed loop control system

S. No	Nature of response parameter	Voltage variation Initial to Final		Ts	Mp	Peak undershoot
1	Transient	0	24	1.8	--	--
2	Set point tracking	24	30	1.5	0.33	0
3	Load disturbance	30	30	1.0	2.83	8.33
4	Source disturbance	30	30	1.5	8.5	4.8

6. CONCLUSION

In summary, PID tuning via the direct synthesis method provides a methodical way to create PID controllers for control systems like boost converters. The required closed-loop transfer function is specified and used to directly calculate the PID gain parameters using the direct synthesis approach. This technique can result in the PID controller being tuned to its maximum potential for a particular control system and the intended performance criteria, such as stability, speed, and accuracy.

The pros and cons of employing direct synthesis PID tuning while developing control systems are covered in this article. Although it can result in high performance and robustness, it necessitates a thorough knowledge of the system and its dynamics as well as substantial computational power. In order to achieve appropriate PID control of complicated systems, such as boost converters, direct synthesis PID tuning is a useful approach.

REFERENCES

1. V. K. Goyal and A. Shukla, "**Two-Stage Hybrid Isolated DC–DC Boost Converter for High Power and Wide Input Voltage Range Applications**," in *IEEE Transactions on Industrial Electronics*, vol. 69, no. 7, pp. 6751-6763, July 2022.

2. M. Veerachary and P. Kumar, "**Analysis and Design of Quasi-Z-Source Equivalent DC–DC Boost Converters**," in *IEEE Transactions on Industry Applications*, vol. 56, no. 6, pp. 6642-6656, Nov.-Dec. 2020.

3. V. K. Goyal and A. Shukla, "**Isolated DC–DC Boost Converter for Wide Input Voltage Range and Wide Load Range Applications**," in *IEEE Transactions on Industrial Electronics*, vol. 68, no. 10, pp. 9527-9539, Oct. 2021.

4. M. Veerachary and A. R. Saxena, "**Optimized Power Stage Design of Low Source Current Ripple Fourth-Order Boost DC–DC Converter: A PSO Approach**," in *IEEE Transactions on Industrial Electronics*, vol. 62, no. 3, pp. 1491-1502, March 2015.

5. M. Y. Bote-Vazquez, E. S. Estevez-Encarnacion, J. Ramirez-Hernandez, L. Hernandez-Gonzalez and O. U. Juarez-Sandoval, "**Predictive Current Control Design Methodology for DC-DC Basic Topologies: Buck, Boost and Buck-Boost Converters**," *2021 IEEE International Autumn Meeting on Power, Electronics and Computing (ROPEC)*, Ixtapa, Mexico, 2021, pp. 1-6.

6. N. Hinov and T. Hranov, "**Model-Based Optimisation of a Buck-Boost DC-DC Converter**," *2020 21st International Symposium on Electrical Apparatus & Technologies (SIELA)*, Bourgas, Bulgaria, 2020, pp. 1-5.

7. G. Marsala and A. Ragusa, "**Heuristic optimization methods applied to improve the performance of controlled DC-DC high boost converter with coupled inductors**," *2016 19th International Conference on Electrical Machines and Systems (ICEMS)*, Chiba, Japan, 2016, pp. 1-6.

8. I. Mandourarakis and E. Koutroulis, "**Optimal design of a boost-type DC-DC converter for PV power-supplied wireless sensor networks**," *2015 IEEE International Conference on Industrial Technology (ICIT)*, Seville, Spain, 2015, pp. 1100-1105.

9. J. D. Kumar, K. Mantosh, M. S. Bhaskar, P. Sanjeevikumar, J. B. Holm Nielsen and Z. Leonowicz, "**Investigation Studies of DC-DC Boost Converter With Proportional-Integral-Derivative Controller Using Optimization Techniques**," *2020 IEEE International Conference on Environment and Electrical Engineering and 2020 IEEE Industrial and Commercial Power Systems Europe (EEEIC / I&CPS Europe)*, Madrid, Spain, 2020, pp. 1-5.